Supporting information

Figure S1. Concentration cell for oxygen transport number measurement.

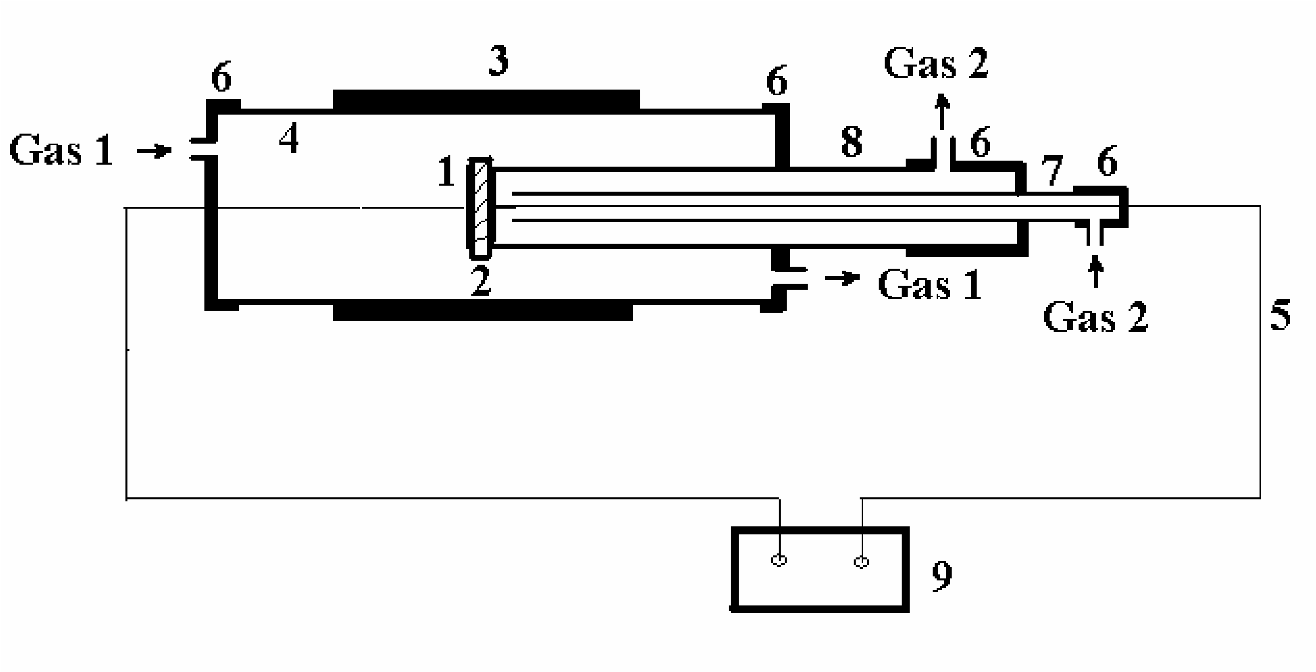

1. Pt electrode; 2. Sample; 3. Tube furnace; 4. alumina tube, 5, Pt wire; 6. Ultra-Torr® vacuum fitting;

7. Inner alumina tube; 8, Outer alumina tube; 9, Electrometer.

Figure S2. Hydrogen-reduction TGA data for as-synthesized $Ba_7Y_2Mn_3Ti_2O_{20}$. The composition determined from the TGA data is $Ba_7Y_2Mn_3Ti_2O_{20.0(1)}$ assuming Mn is reduced to +2 and Ti stays as +4 in the final product. The initial mass loss below 200 °C is assigned to loss of water.

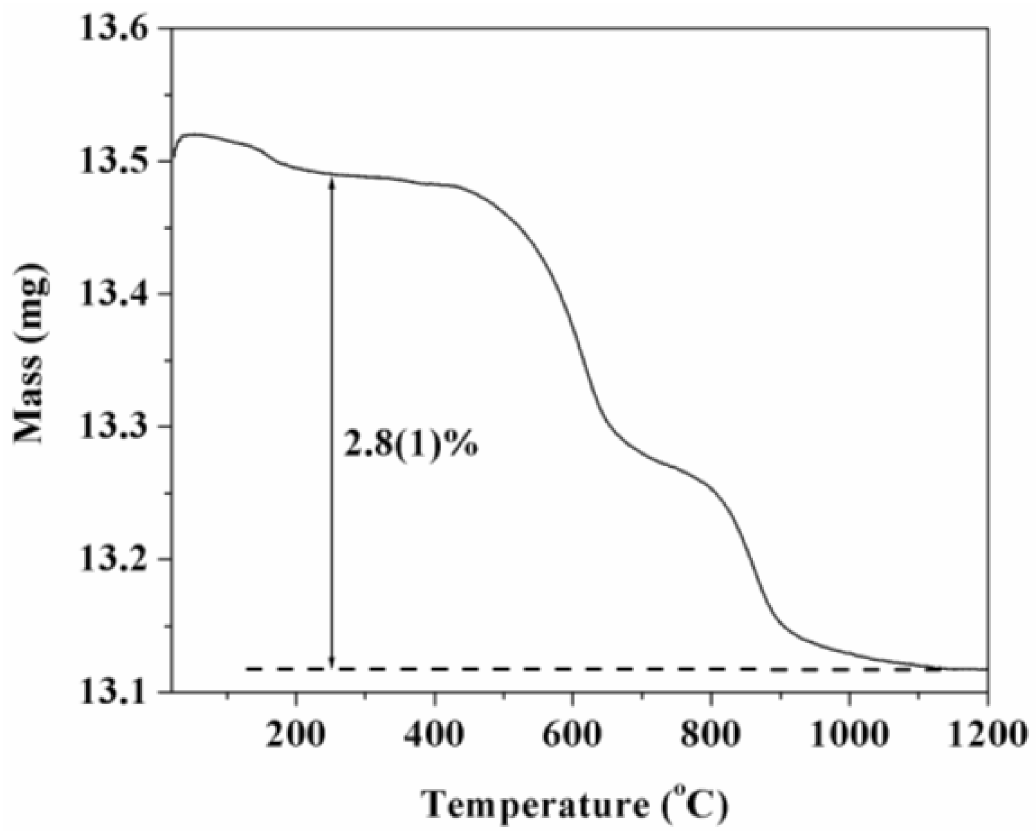

Figure S3. Rietveld refinement of XRD data for as-synthesized $Ba_7Y_2Mn_3Ti_2O_{20}$.

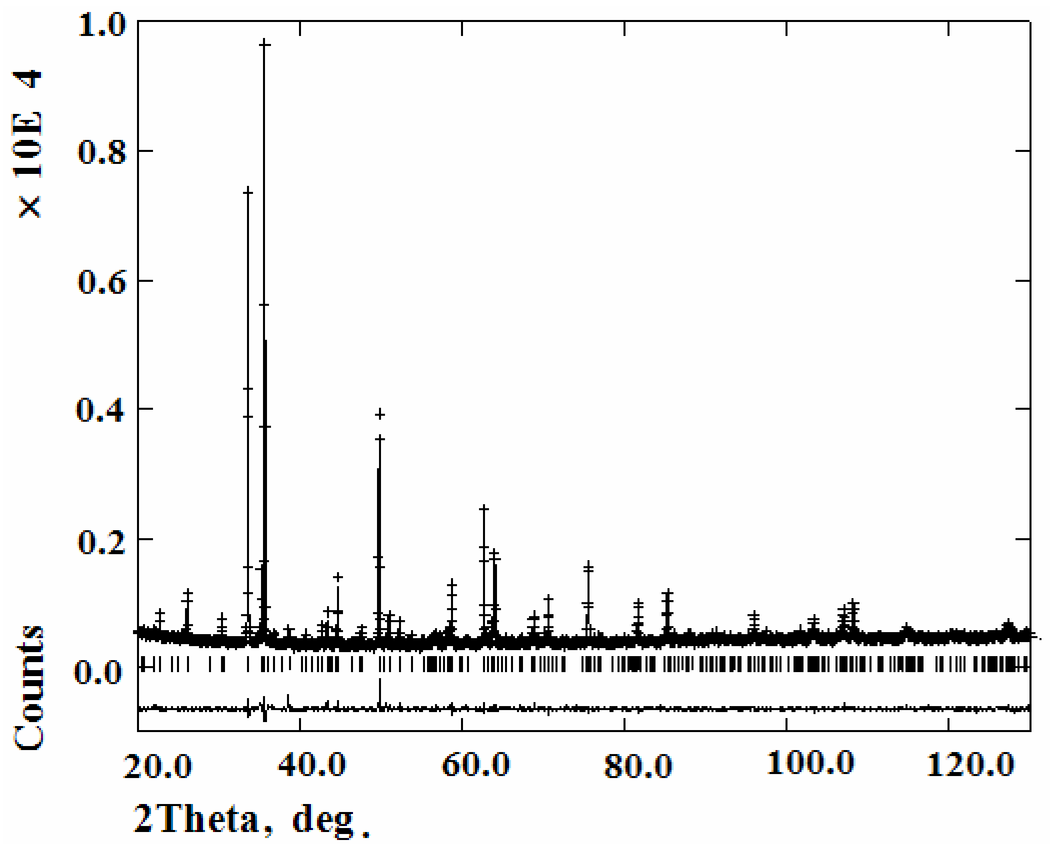

Figure S4. z = 0 sections of the difference Fourier map with all atoms except for O4 for the as-synthesized (a) and reduced (b) $Ba_7Y_2Mn_3Ti_2O_{20}$ sample 1 at ambient temperature, re-plotted by using MAPVIEW in the WINGX software package.

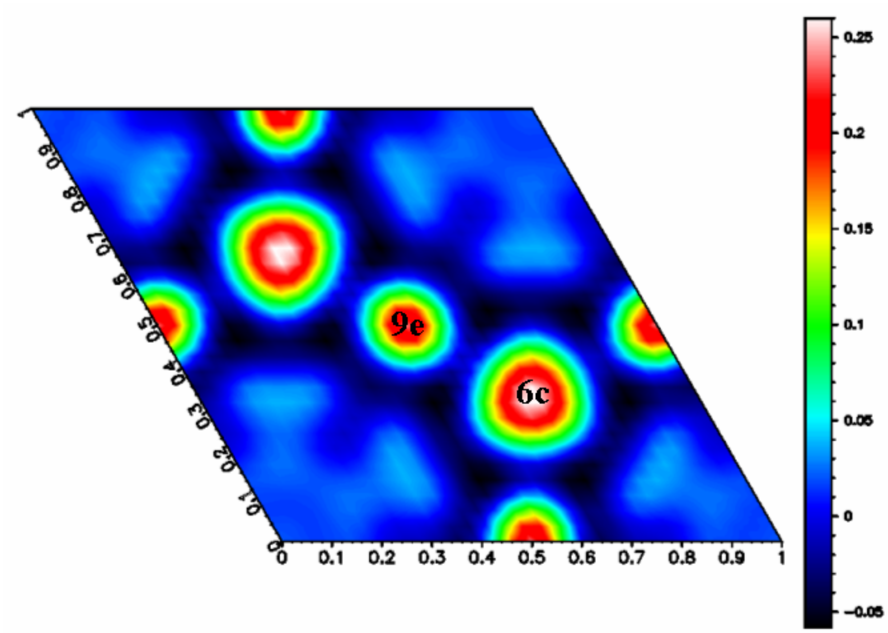

(a)

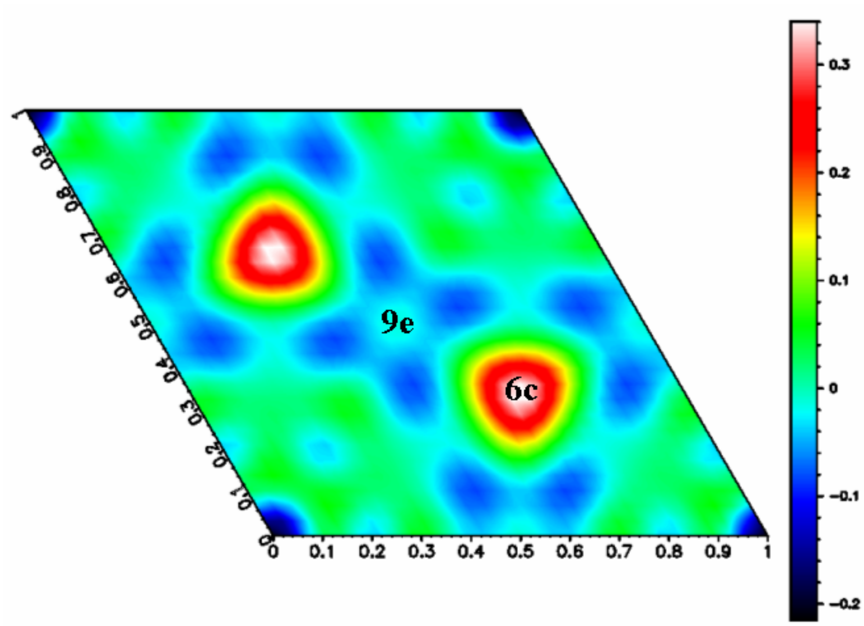

(b)

Table S1. Ba-O Bond lengths (Å) for as-synthesized $Ba_7Y_2Mn_3Ti_2O_{20}$ sample 1 at ambient temperature.

Bond	Length	Bond	Length	Bond	length
Ba1'-O2 (×6)	2.869(2)	Ba2-O1 (×3)	3.062(3)	Ba4-O1 (×3)	2.829 (3)
Ba1'-O4 (×3)	3.036(9)	Ba2-O3 (×3)	2.9320(3)	Ba4-O2 (×3)	2.9372(4)
Ba1'-O4 (×3)	3.43(1)	Ba2-O3 (×3)	2.9314(3)	Ba4-O2 (×3)	2.9378(4)
BVS for Ba1'	1.77	Ba2-O3 (×3)	2.932(3)	Ba4-O4 (×0.616)	2.512(7)
Ba1"-O2 (×3)	2.73(2)	BVS for Ba2	1.93	Ba4-O5 (×0.192) [a]	3.16(2)
Ba1"-O2 (×3)	3.02(2)	Ba3-O1 (×3)	2.9427(5)	Ba4-O5 (×0.192) [a]	3.05(2)
Ba1"-O5 (×2)	2.90(7)	Ba3-O1 (×3)	2.9433(5)	BVS for Ba4	2.09
Ba1"-O5 (×2)	2.88(8)	Ba3-O2 (×3)	3.417(4)		
BVS for Ba1"	2.11	Ba3-O3 (×3)	2.741(3)		
		BVS for Ba3	2.03		

Table S2. Ba-O Bond lengths (Å) for the reduced $Ba_7Y_2Mn_3Ti_2O_{20}$ sample 1 at ambient temperature.

Bond	Length	Bond	Length
Ba1-O2 (×6)	2.879(3)	Ba3-O1 (×3)	2.9534(7)
Ba1-O4 (×3)	3.39(1)	Ba3-O1 (×3)	2.9540(7)
Ba1-O4 (×3)	3.031(9)	Ba3-O2 (×3)	3.460(5)
BVS for Ba1	1.76	Ba3-O3 (×3)	2.729(4)
Ba2-O1 (×3)	3.082(5)	BVS for Ba3	2.01
Ba2-O3 (×3)	2.9397(4)	Ba4-O1 (×3)	2.833(4)
Ba2-O3 (×3)	2.9391(4)	Ba4-O2 (×3)	2.9471(6)
Ba2-O3 (×3)	2.918(4)	Ba4-O2 (×3)	2.9465(6)
BVS for Ba2	1.91	Ba4-O4 (×1)	2.578(6)
		BVS for Ba4	2.14

Table S3. Final structural parameters for unsealed $Ba_7Y_2Mn_3Ti_2O_{20}$ sample 1 at 873 K under dynamic vacuum.

atom	site	x	y	z	U_{iso} (Å^2)	Occupancy
Ba1	3a	0	0	0	0.0100(5)	1
Ba2	6c	0	0	0.14643(8)	0.0100(5)	1
Ba3	6c	0	0	0.22834(8)	0.0100(5)	1
Ba4	6c	0	0	0.38445(7)	0.0100(5)	1
Y	6c	0	0	0.07380(6)	0.82(6)	1
M1	3b	0	0	0.5	0.0037(7)	1 unit [a]
M2	6c	0	0	0.6978(1)	0.0037(7)	1 unit [a]
M3	6c	0	0	0.4501(1)	0.0037(7)	1 unit [a]
O1	18h	0.1782(2)	0.8218(2)	0.09742(3)	0.0137(6)	1
O2	18h	0.4956(3)	0.5044(3)	0.37869(4)	0.0259(6)	1
O3	18h	0.1471(2)	0.8529(2)	0.47641(3)	0.0076(4)	1
O4	36i	0.007(3)	-0.064(2)	0.33489(9)	0.025(3)	1/6

Space group: $R\bar{3}m$, a = 5.89722(2)Å, c =51.3659(3)Å, Z = 3. R_{wp} = 5.41%, R_p = 4.76%, χ^2 = 1.64 for 40 variables, R_F^2 = 8.91%. [a]:1 unit = 0.6Mn/0.4Ti.

Table S4. Selected atomic distances (Å) and angles (degree) for unsealed $Ba_7Y_2Mn_3Ti_2O_{20}$ sample-1 at 873 K under dynamic vacuum.

Bond	Bond length	Bond	Bond length/angle
Ba1-O2 (×6)	2.912(2)	Ba4-O4 (×6) [a]	2.577(6)
Ba1-O4 (×12) [a]	3.39(1)	Y-O1 (×3)	2.188(3)
Ba1-O4 (×12) [a]	3.09(1)	Y-O2 (×3)	2.277(4)
Ba2-O1 (×3)	3.106(4)	M1-O3 (×6)	1.931(2)
Ba2-O3 (×3)	2.9606(3)	M2-O2 (×3)	1.812(4)
Ba2-O3 (×3)	2.9601(3)	M2-O4 (×6) [a]	1.724(7)
Ba2-O3 (×3)	2.947(3)	Ba4-M2	4.222(8)
Ba3-O1 (×3)	2.9762(6)	M3-O1 (×3)	1.871(4)
Ba3-O1 (×3)	2.9768(6)	M3-O3 (×3)	2.020(4)
Ba3-O2 (×3)	3.483(4)	M1-M3	2.562(5)
Ba3-O3 (×3)	2.728(4)	O2-M2-O2 (×3)	104.8(2)
Ba4-O1 (×3)	2.858(4)	O2-M2-O4 (×1)	125.9(3)
Ba4-O2 (×3)	2.9640(4)	O2-M2-O4 (×1)	111.9(5)
Ba4-O2 (×3)	2.9635(4)	O2-M2-O4 (×1)	102.7(4)

Figure S5. The complex impedance Z"-Z' plot, Y'-*f* and C'-*f* bode plots for a $Ba_7Y_2Mn_3Ti_2O_{20}$ pellet at 398 K. The experimental and calculated data are shown as blue open square and red solid line respectively.

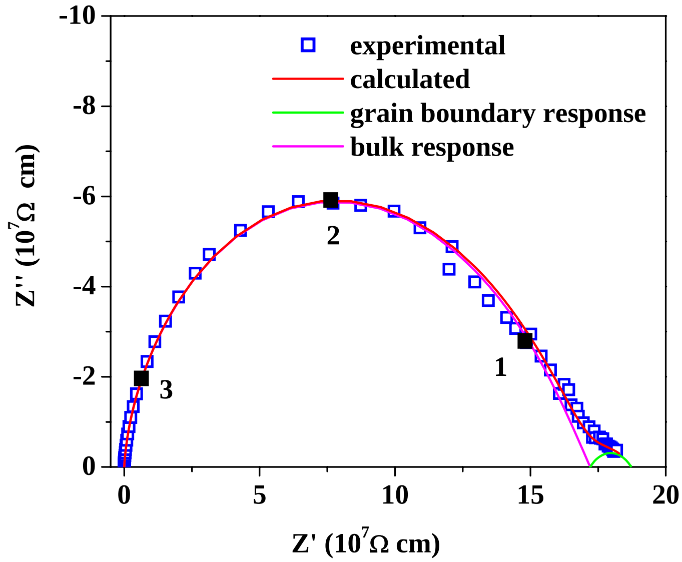

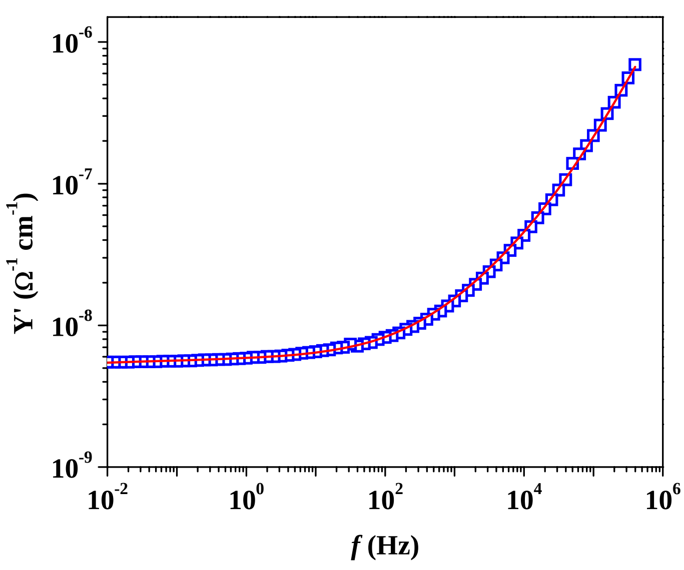

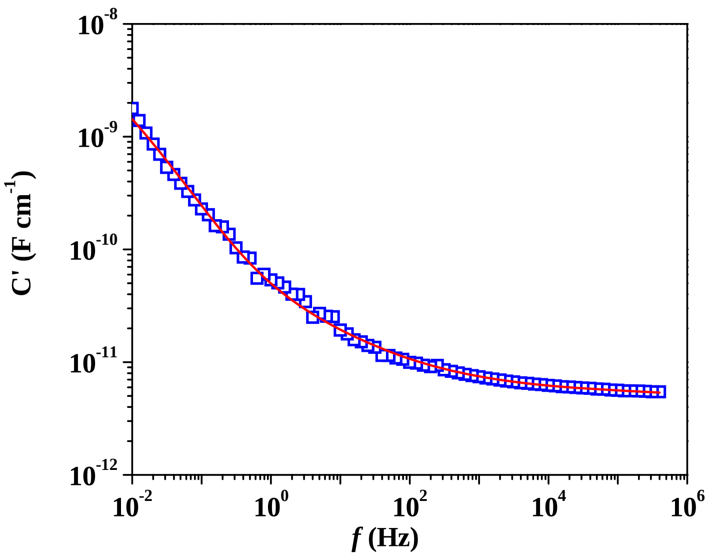

Figure S6. The pO_2 dependence of bulk conductivity of a $Ba_7Y_2Mn_3Ti_2O_{20}$ pellet at 873 K.

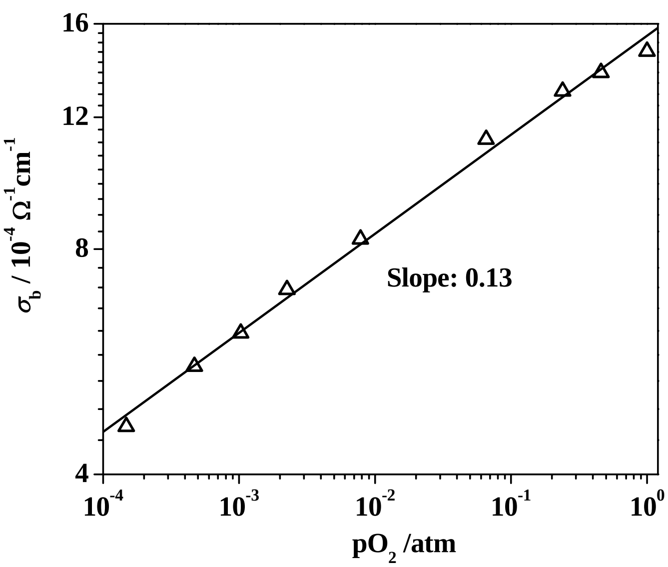

Figure S7. Infrared absorption spectrum of $Ba_7Y_2Mn_3Ti_2O_{20}$ (a) and $Ba_7Ca_2Mn_5O_{20}$ (b).